Journal Pre-proof

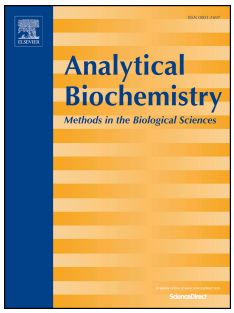

Rapid and sensitive detection of *Salmonella* with reduced graphene oxide-carbon nanotube based electrochemical aptasensor

Jimmy Nelson Appaturi, Thiruchelvi Pulingam, Kwai Lin Thong, Shalini Muniandy, Noraini Ahmad, Bey Fen Leo

PII: S0003-2697(19)30657-8

DOI: https://doi.org/10.1016/j.ab.2019.113489

Reference: YABIO 113489

To appear in: *Analytical Biochemistry*

Received Date: 7 July 2019

Revised Date: 19 October 2019

Accepted Date: 22 October 2019

Please cite this article as: J.N. Appaturi, T. Pulingam, K.L. Thong, S. Muniandy, N. Ahmad, B.F. Leo, Rapid and sensitive detection of *Salmonella* with reduced graphene oxide-carbon nanotube based electrochemical aptasensor, *Analytical Biochemistry* (2019), doi: https://doi.org/10.1016/j.ab.2019.113489.

Rapid and sensitive detection of *Salmonella* with reduced graphene oxide-carbon nanotube based electrochemical aptasensor

Jimmy Nelson Appaturi[a], Thiruchelvi Pulingam[b], Kwai Lin Thong[c], Shalini Muniandy[b], Noraini Ahmad[d], Bey Fen Leo[b, e ,1]

[a]*SM Pharmaceuticals SDN BHD; Lot 88, Sungai Petani Industrial Estate, Sungai Petani, 08000 Kedah, Malaysia.*
[b]*Nanotechnology & Catalysis Research Centre (NANOCAT), Institute of Advanced Studies, University of Malaya, 50603 Kuala Lumpur, Malaysia.*

[c]*Institute of Biological Science, Faculty of Science, University of Malaya, 50603, Kuala Lumpur, Malaysia*

[d]*Department of Chemistry, Faculty of Science, University of Malaya, 50603 Kuala Lumpur, Malaysia*

[e] *Faculty of Medicine, University of Malaya, 50603 Kuala Lumpur, Malaysia*

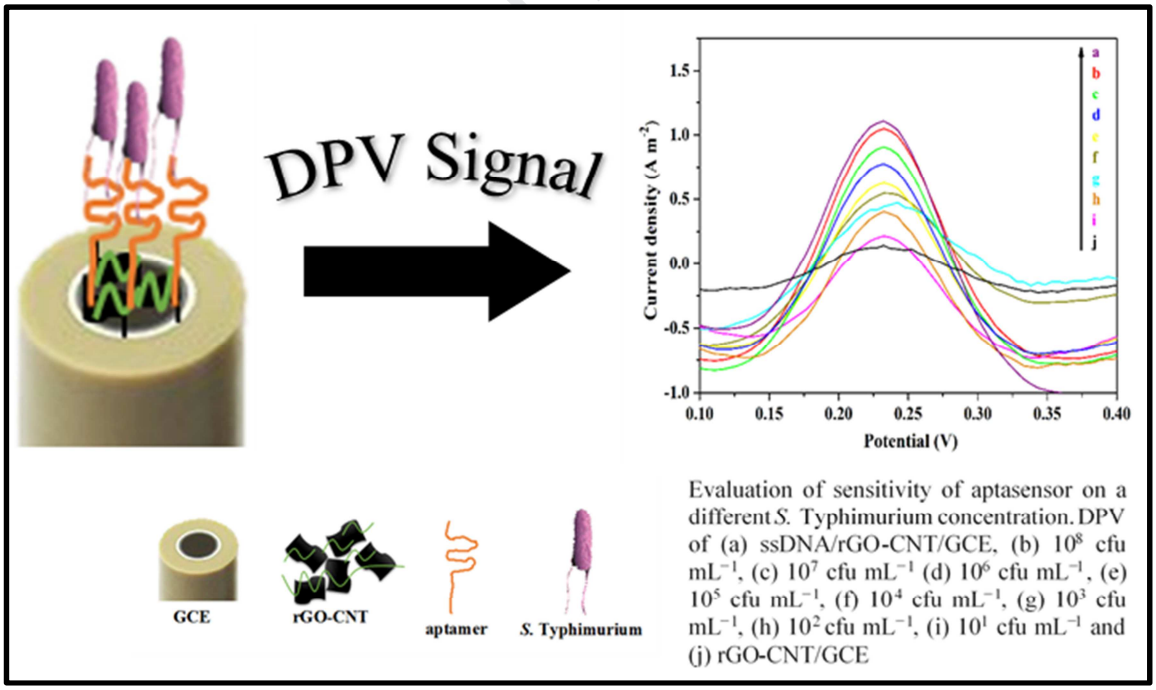

Evaluation of sensitivity of aptasensor on a different *S.* Typhimurium concentration. DPV of (a) ssDNA/rGO-CNT/GCE, (b) 10^8 cfu mL^{-1}, (c) 10^7 cfu mL^{-1} (d) 10^6 cfu mL^{-1}, (e) 10^5 cfu mL^{-1}, (f) 10^4 cfu mL^{-1}, (g) 10^3 cfu mL^{-1}, (h) 10^2 cfu mL^{-1}, (i) 10^1 cfu mL^{-1} and (j) rGO-CNT/GCE

[1] Corresponding author.
E-mail address: beyfenleo@um.edu.my (B.F. Leo)

Rapid and sensitive detection of *Salmonella* with reduced graphene oxide-carbon nanotube based electrochemical aptasensor

Jimmy Nelson Appaturi[a], Thiruchelvi Pulingam[b], Kwai Lin Thong[c], Shalini Muniandy[b], Noraini Ahmad[d], Bey Fen Leo[b, e ,*]

[a]*SM Pharmaceuticals SDN BHD; Lot 88, Sungai Petani Industrial Estate, Sungai Petani, 08000 Kedah, Malaysia.*
[b]*Nanotechnology & Catalysis Research Centre (NANOCAT), Institute for Advanced Studies, University of Malaya, 50603 Kuala Lumpur, Malaysia.*

[c]*Institute of Biological Science, Faculty of Science, University of Malaya, 50603, Kuala Lumpur, Malaysia*

[d]*Department of Chemistry, Faculty of Science, University of Malaya, 50603 Kuala Lumpur, Malaysia*

[e] *Faculty of Medicine, University of Malaya, 50603 Kuala Lumpur, Malaysia*

Abstract

Rapid detection of foodborne pathogens is crucial as ingestion of contaminated food products may endanger human health. Thus, the objective of this study was to develop a biosensor using reduced graphene oxide-carbon nanotubes (rGO-CNT) nanocomposite *via* the hydrothermal method for accurate and rapid label-free electrochemical detection of pathogenic bacteria such as *Salmonella enterica.* The rGO-CNT nanocomposite was characterized using Fourier transform infrared spectroscopy, Raman spectroscopy, X-ray diffraction and transmission electron microscopy. The nanocomposite was dropped cast on the glassy carbon electrode and further modified with amino-modified DNA aptamer. The resultant ssDNA/rGO-CNT/GCE aptasensor was then used to detect bacteria by using differential pulse voltammetry (DPV) technique. Synergistic effects of aptasensor was evident through the combination of enhanced electrical properties and facile chemical functionality of both rGO and CNT for the stable interface. Under optimal experimental conditions, the aptasensor could detect *S.* Typhimurium in a wide linear dynamic range from 10^1 until 10^8 cfu mL^{-1} with a 10^1 cfu mL^{-1} of the limit of detection. This aptasensor also showed good sensitivity, selectivity and specificity for the detection of microorganisms. Furthermore, we have successfully applied the aptasensor for *S.* Typhimurium detection in real food samples.

Keywords: Aptasensor; Aptamer; Reduced Graphene Oxide; Carbon nanotubes; *Salmonella*

* Corresponding author.
E-mail address: beyfenleo@um.edu.my (B.F. Leo)

1 Introduction

Salmonella enterica is a major foodborne pathogen causing foodborne illnesses globally, including Asian countries such as Singapore, Malaysia, Japan and Thailand [1]. In Malaysia, 48.51 cases of *Salmonella* associated foodborne illnesses per 100,000 people have been reported by the Ministry of Health, Malaysia [2]. *Salmonella enterica* is mainly transmitted through consumption of contaminated raw or uncooked food products (e.g. vegetables, fruits, poultry, meat and eggs) and may cause serious risk to consumers' health [3]. Lack of hygiene practice in production, handling and transportation of food products could lead to easy contamination with *Salmonella*. The increasing numbers of food poisoning cases due to *Salmonella enterica* implied that there is a crucial need for a more sensitive and rapid detection method to detect and quantitate the presence of this pathgoen in food products [4]. Early detection of *Salmonella* in the food chain will help to prevent the spread of nontyphoidal salmonellosis [5].

Among the *Salmonella enterica*, *S.* Typhimurium is the most common serovar associated with food poisoning outbreaks in humans. Methods that are routinely used for the detection of *S.* Typhimurium include culture-based methods, PCR-based assays or immunoassays that are usually time-consuming, costly, require skilled personnel and sophisticated instruments [4]. Therefore, there is a concerted effort to develop alternative approach such as biosensors which are rapid, sensitive and accurate in detecting *S.* Typhimurium [6]. Although there are several types of biosensors, the electrochemical-based biosensors are favoured due to their low cost, miniaturization capacity, sustainability and minimal use of reagents and samples [7]. Furthermore, the use of aptamers in the electrochemical-based biosensor platform further improves sensitivity and affinity as aptamers are highly specific towards target molecules [8].

DNA or RNA aptamers are single-stranded oligonucleotides and highly selective towards the target molecule [9]. Typically, the aptamers are selected through an *in vitro* method referred to as SELEX (Systemic Evolution of Ligands by EXponential enrichment) [10]. The benefits of aptamer usage include easy modification, low cost, fast synthesis and its stability. Moreover, aptasensors (aptamer-based biosensors) have been coupled with an electrochemical-based platform to facilitate detection of pathogens and quantification especially for food safety requirements [1,11] This aptasensor is very useful and highly desirable because of its high productivity, low limit of detection, simplicity portability and most importantly, it requires a low volume of analytes [12]. Several aptamer sequences have been designed for the detection of various target bacteria including *S.* Typhimurium, *Staphylococcus aureus*, *Vibrio parahaemolyticus*, *Listeria monocytogenes* and *Shigella dysenteriae* [13,11]. The aptamer sequence used in this study was designed by Joshi *et al*. to complement an outer membrane protein that is found on *S.* Typhimurium as the specific binding target [14].

Excellent physicochemical attributes of carbon-based nanomaterials enhanced the increasing use of these materials as a component in biosensors [15]. Specifically, high electrical conductivity and enhanced surface area of carbon-based nanomaterials in combination with aptamers as the recognition element improve the overall sensitivity of the aptasensors [16]. Graphene, a carbon-based nanomaterial, has emerged as an attractive nanomaterial in the field of electrochemical application mainly due to its excellent electrical and thermal conductivity [17]. However, the methods of graphene synthesis which include chemical vapor deposition and mechanical exfoliation are too costly and produce low yield [18]. Therefore, chemical or hydrothermal reduction of graphene oxide to generate reduced graphene oxide (rGO) has become an inexpensive procedure to imitate qualities of pristine graphene with similar mechanical and electronic properties [19]. Properties of rGO such as

increased current density and chemical inertness along with biocompatibility facilitate rGO surface modification through hydrogen bonding or π-π stacking [20,21]. Yet, less than optimal performances have been noted for rGO due to interlayer effects of van der Waals interactions which reduce the total surface area of rGO due to the restacking of graphene sheets [22]. Therefore, the hybridization of rGO with carbon nanotubes (CNT) has prevented the aggregation of graphene sheets as CNT acts as a one-dimensional spacer between the sheets [23]. Additionally, high surface area and excellent electrical conductivity of CNT further complement rGO for sensing purpose. The increased surface area in rGO-CNT hybrid nanocomposite allows covalent binding between the carboxyl group of the rGO-CNT and amino-modified aptamers, resulting in a highly stable and sensitive aptasensor [24].

The rGO-CNT has been developed recently as an aptasensor by some researchers to detect the biomarker prostate specific antigen in serum [25], breast cancer biomarker HER2 [26] and lysozyme [27]. Previously, we developed an electrochemical aptasensor using rGO-azophoxine which exhibited a wide detection range from 10^1 to 10^8 cfu mL^{-1} for *S.* Typhimurium [1]. The physicochemical characteristics of rGO such as high electrical and thermal conductivity, and the fibrous structure of CNT with the ability to mediate electrons and act as an immobilization matrix prompted us to investigate the aptasensing ability of the rGO-CNT nanocomposite. Hence, the present work focuses on the synthesis and development of hybrid rGO-CNT nanocomposite and amino-modified aptamer as a sensitive electrochemical sensing platform for detecting *S.* Typhimurium, a major foodborne disease-causing pathogen.

The rGO-CNT aptasensor was designed using the hybridization technique between rGO and CNT without any chemical reduction method and dropped-cast onto glassy carbon electrode (GCE). In this study, amino-modified aptamer was used as a linker to ensure the binding between rGO-CNT-aptamer-bacteria. Under the optimal conditions, the aptasensor

could detect the *S.* Typhimurium *via* differential pulse voltammetry (DPV) technique. Furthermore, the aptasensor was also applied to detect the foodborne pathogen in real chicken samples. The developed aptasensor has several distinct advantages including high sensitivity, good selectivity and low cost. This study is the first to report the application of ssDNA/rGO-CNT/GCE as an aptasensor for detecting *Salmonella*.

2 Experimental

2.1 Materials and reagents

Graphite powder, Phosphoric acid (85 %), Nitric acid (65 %) Hydrochloric acid (37 %), Sulfuric acid (98 %), Potassium permanganate, Potassium ferricyanide, Hydrogen peroxide (30 %), 10 X Phosphate Buffer Saline (PBS), Potassium chloride and CNT were purchased in analytical grade from Sigma-Aldrich. The *Salmonella enterica* serovars that were used included *S.* Typhimurium (model organism), *S.* Enteritidis, *S.* Albany, *S.* Weltevreden, *S.* Typhi, and *S.* Derby while non-*Salmonella* bacterial species were represented by *Escherichia coli*, *Klebsiella pneumoniae*, *Pseudomonas aeruginosa*, *Staphylococcus aureus* and *Enterococcus faecalis*. All the bacterial strains used in this work were from the Biomedical Science Laboratory, University of Malaya, Kuala Lumpur, Malaysia. DNA sequence of the aptamer (recognition biomolecule) was as previously published [28].

2.2 Instrumentation

The functional groups of the GO, rGO, CNT and rGO-CNT were determined by Fourier transform infrared (FT-IR) (Bruker IFS 66V/S, USA), whereas the Raman analysis was done through Renishaw inVia Raman microscope, Gloucestershire, UK. The X-ray diffraction (XRD) study was conducted using X-ray diffractometer (Bruker d8 ADVANCE). The morphology of the prepared nanocomposite was characterized using a transmission electron microscope (TEM, LEO LIBRA 120, Carl Zeiss). The electrochemical experiments were

performed using PGSTAT302N (Metrohm AG, Switzerland), an electrochemical workstation. Three-electrode system was used along with GCE, the working electrode, a platinum wire, the counter electrode and silver/silver chloride (Ag/AgCl), the reference electrode. Exfoliation of GO was conducted using Ultrasonic bath sonicator. Centrifugation (HITACHI CR22N, Japan) and homogenization (IKA RW20 digital Homogenizer) methods were carried out to produce GO in the form of a slurry and the whole process was conducted in a fumehood (LABCONCO Protector Laboratory Hood). All bacterial culture work was carried out in a Biosafety cabinet (ESCO Streamline SC2-6A1).

2.3 Preparation of rGO-CNT

Graphene oxide (GO) was synthesized through a modified Hummers procedure [29,11]. In order to obtain a purified carbon nanotube (CNT), the CNT powder that was impurified (100 mg) was left to heat at 480 ºC in the atmospheric pressure and followed by a 12 h of reflux using 3 mol L^{-1} HNO_3/HCl solution to eliminate metal oxides [30]. The treated CNT was then washed and filtered a few times using deionized water until a neutral pH was measured. Reduced graphene oxide (rGO) was then prepared using the GO. In a typical preparation process, 30 mg of GO was suspended in 15 mL ethylene glycol and was sonicated for 1 h till it became a brown colloidal solution.

Then, the solution was sealed using Teflon-lined autoclave and was heated in an oven for 18 h at 180 °C. The solids were washed with acetone and followed by distilled water to remove the additional GO. Finally, the rGO were dried in an oven (65 °C, 24 h). The rGO-CNT composites were then prepared by a hydrothermal method. In a typical procedure, a mixture of 10 mg of rGO and 10 mg of CNT was dispersed in distilled water and sonicated with a probe (Ultrasonic processor FS-250N, Shanghai, China). After a homogeneous black-brown dispersion was obtained, the mixture was shifted into a Teflon-lined autoclave, then

heated in an oven (180 °C, 24 h). Once it had cooled to room temperature, the resulting suspension was centrifuged to collect the precipitate. Finally, the composites were further washed 5 times with acetone and distilled water to remove the excess rGO and CNT.

2.4 Bacterial cultures

S. Typhimurium strain was cultured in Luria-Bertani broth for 24 hr with constant shaking. Bacterial cells from the overnight bacterial culture were harvested through centrifugation step at 5000 rpm for approximately 10 min. The cell pellets were washed once with 1X PBS (0.1M, pH 7.4) to remove traces of growth media. The bacterial cells were then resuspended in 1 mL of 1X PBS solution and diluted 10-folds to reach concentrations of 10^1 to 10^8 cfu mL^{-1}. The cell density of each dilution was then confirmed through conventional culture plating method. The procedure was repeated for *S.* Albany, *S.* Enteritidis, *S.* Weltevreden, *S.* Typhi, *S.* Derby, *E. coli*, *K. pneumoniae*, *P. aeruginosa*, *S. aureus* and *E. faecalis*.

2.5 Modification of the ssDNA/rGO-CNT/GCE aptasensor

GCE was initially polished using 0.05 µm-sized alumina fine powder to remove impurities from the electrode surface, and the electrode was then ultrasonicated, rinsed with distilled water and then left to dry at room temperature. For the modification of ssDNA/rGO-CNT/GCE aptasensor, firstly, 10 µL of the rGO-CNT suspension was dropped-cast on GCE surface and was left to dry under ambient conditions. Then, 5 µL of 5 µmol L^{-1} of the amino-modified *Salmonella* aptamer was then dropped on the surface of the rGO-CNT/GCE and air-dried at room temperature to obtain ssDNA/rGO-CNT/GCE aptasensor. The fabricated electrode was then stored at 4 °C until future use. The overall modification process is schematically shown in Fig. 1.

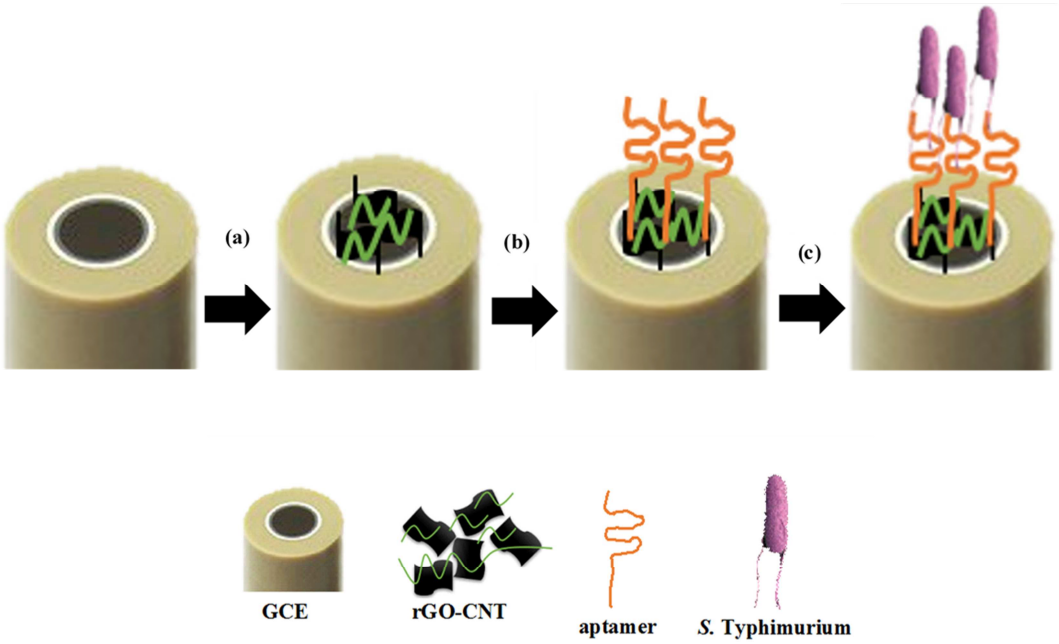

Fig. 1. A schematic diagram of the modification process of GCE. a) drop casting of rGO-CNT on GCE, b) rGO-CNT/GCE modified with amino-aptamer, c) ssDNA/rGO-CNT/GCE incubation with *S.* Typhimurium.

2.6 Analysis of the working electrodes through electrochemical method

CV technique was applied to determine the electrical conductivity of bare GCE, rGO/GCE, rGO-CNT/GCE and ssDNA/rGO-CNT/GCE using Zobell's solution (0.1 mol L^{-1} of KCl solution containing 3 mmol L^{-1} of $K_3[Fe(CN)_6]$) at 100 mVs^{-1}scan rate. To optimize the condition of the sensing platform, the effects of rGO-CNT with concentrations ranging from 1 to 11 mg mL^{-1} and the aptamer concentrations (1 to 20 µmol L^{-1}) were also studied using CV.

To quantitate the presence of S. Typhimurium, the aptasensor was incubated with different concentrations of bacterial cultures ranging from 10^1 until 10^8 cfu mL^{-1} for approximately 5 min in PBS solution. Then, the corresponding DPV was carried out in Zobell's solution (electrolyte) at 6 mVs^{-1} scan rate. For the comparison studies, the DPV of ssDNA/rGO-CNT/GCE and rGO-CNT/GCE without any bacteria incubation were tested. To determine the

selectivity and specificity of the aptasensor, another five serovars of *Salmonella enterica* (*S.* Albany, *S.* Enteritidis, *S.* Weltevreden, *S.* Typhi and *S.* Derby) and five non-*Salmonella* bacteria such as *E. coli, K. pneumoniae, P. aeruginosa, S. aureus* and *E. faecalis* were cultured as previously mentioned. A standard concentration of 10^2 cfu mL^{-1} of each culture was used for the test. All the electrochemical measurements were done in a clean environment in the Biosafety cabinet (ESCO Streamline SC2-6A1).

2.7 Aptasensor evaluation using food samples

The developed aptasensor was further evaluated using raw chicken meat sample (n = 5) purchased from a supermarket. Approximately 10 g of chicken meat was homogenized using 90 mL of buffer peptone water (BPW) for 3 hr at 37 ºC. The pre-enriched food sample homogenate was then centrifuged, and the remaining cell pellet was resuspended in the PBS buffer. The cell suspension was serially diluted 10-folds. The colony forming units of the diluted bacterial suspension was determined through viable plating method on Brilliance™ Agar for *Salmonella* isolation (Oxoid). In parallel, an aliquot of 1 mL of pre-enriched food sample homogenate (in PBS buffer) was used to evaluate the working of the aptasensor. The food homogenate was left at room temperature for 5 min prior to electrochemical detection. For each food sample, three consecutive tests were carried out to confirm the reproducibility of the results.

3 Results and discussion

3.1 Surface characterization of rGO and rGO-CNT

The interaction between rGO and CNT was studied using FT-IR spectra. Fig. 2(a) shows the FT-IR spectra of GO, rGO, CNT and rGO-CNT. Based on FT-IR spectrum of GO, several peaks that corresponded to C=O stretching at 1724 cm^{-1}, C–O–C stretching at 1391 cm^{-1}, and C–O stretching at 1082 cm^{-1} were reduced or absent in the rGO [1]. This

observation clearly indicated that the GO has been partially reduced by the decomposition method. Due to the partially reduced GO, the peak corresponding to the -OH functional groups remained in the rGO which help to interact with CNT. In rGO spectrum, the broad band at ~3253 cm^{-1} corresponded to the hydroxyl group (-OH). Interestingly, this band was slightly shifted to ~3204 cm^{-1} and was shrunken after the functionalization of CNT. There are three possibilities the existence of hydroxyl group (-OH). Firstly, the initial GO already contain huge amount of -OH groups shown by the shoulder at around 3200 cm^{-1} appears in the green spectrum. So, the reduction using the ethylene glycol (EG) only reduces carboxylic acid groups and not hydroxyl group. This was supported by the disappearance of 1724 cm^{-1} signal. Secondly, the use of EG under thermal condition only partially reduce the GO, not as good as strong acids. Finally, EG substance is quite hygroscopic and able to hold water. The presence of the broad signal maybe also due to the wet condition and trace amount of EG in the rGO sample.

In the FT-IR spectrum of rGO, the band at 1631 cm^{-1} can be attributed to the C=C stretching which is present due to sp^2 hybridization being shifted to 1557 cm^{-1} in rGO-CNT. Moreover, the peak at 2340 cm^{-1} which is found in rGO-CNT can be related to the presence of carbon dioxide (CO_2). CO_2 cannot be eliminated as it can be presence in all samples. This was also supported by the missing 1724 cm^{-1} and 3400 cm^{-1} signals. The C-O-C stretching vibrations in rGO-CNT are shown in the two absorption peaks at about 1323 cm^{-1} and 1027 cm^{-1}. Since this is partial reduction, C-O-C is possible especially condensation of adjacent -OH groups. All these FT-IR bands present in rGO-CNT provided direct evidence of a successful immobilization of rGO and CNT.

The results of the Raman spectroscopy further elucidate the vibration bands of the rGO and rGO-CNT nanocomposite. Fig. 2(b) shows Raman spectra of the GO, rGO, CNT

and rGO-CNT nanocomposite. The spectrum of rGO showed two significant vibrations at 1310 cm^{-1} (D band) and 1600 cm^{-1} (G band) representing the existence of structural defects in sp^2-hybridized carbon system and first-order scattering of E_{2g} phonons of sp^2 carbon atoms. For rGO-CNT nanocomposite, both D and G bands are shown at 1349 and 1600 cm^{-1} correspondingly and two other peaks of 2D (2690 cm^{-1}) and D+G (2941 cm^{-1}) designated successful incorporation of rGO and CNT. The formation of rGO-CNT nanocomposite increases the peak intensity of D and G bands as compared to rGO peak intensities. However, the individual CNT peak showed the respective D and G bands at higher peak intensities as compared to rGO and rGO-CNT. These differences are due to the decrease of in-plane sp^2 domain sizes resulting from the introduction of oxygen-containing groups and increased defects in its graphitic domains [31].

To further support the FT-IR and Raman studies, the high angle XRD analyses for GO, rGO, CNT and rGO-CNT are depicted in Fig. 2(c). The observed amorphous peak at 2θ of 23.7° corresponds to the (002) reflection plane of rGO which is consistent with the values reported in the literature [32]. The XRD pattern of rGO-CNT nanocomposite has more than one peak which confirms the interaction between rGO and CNT forming a rGO-CNT nanocomposite. The XRD pattern of rGO-CNT had a similar diffracted pattern peak (002) with CNT and rGO sheet. Nevertheless, this peak slightly shifted and appeared as an intense broad peak at 25.4°. In addition, the peak defining in-plane regularity (100) appeared at 2θ = 40.4 shows that the CNT has been successfully incorporated with rGO. There are other small peaks which presence are due to the catalyst that was present during CNT preparation. However, these impurities did not negate the performance of the aptasensor.

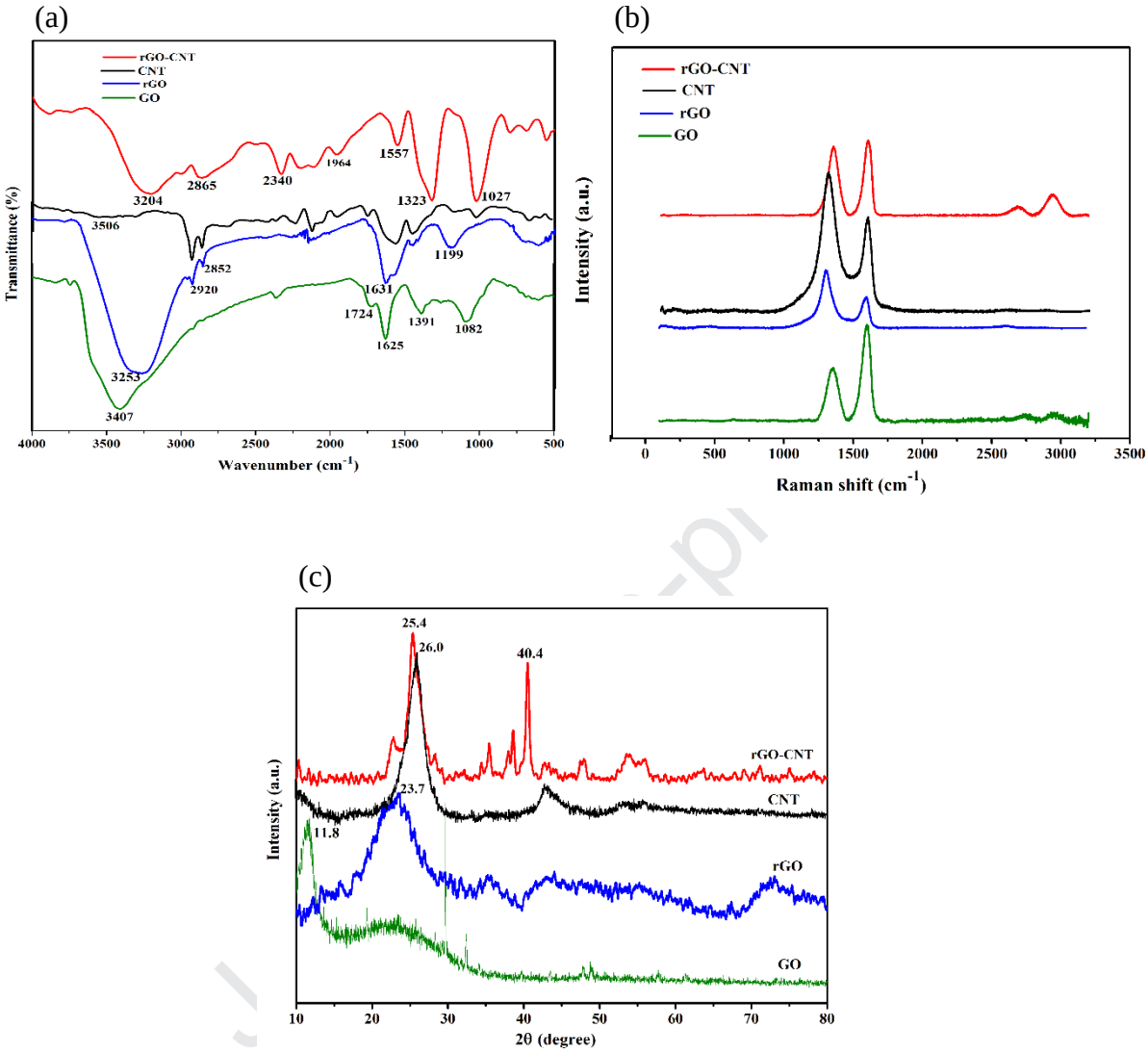

Fig. 2. The (a) FT-IR spectra of GO, rGO, CNT and rGO-CNT, (b) Raman spectra of GO, rGO, CNT and rGO-CNT and (c) High angle XRD pattern of the GO, rGO, CNT and rGO-CNT nanocomposites.

The TEM images of GO, rGO, CNT and rGO-CNT are presented in Fig.3a, 3b, 3c and 3d, respectively. The presence of thin multilayers of graphene oxide nanosheet is clearly demonstrated in Fig.3a. This result further supports the Raman data. As can be seen from Fig.

3b, the surface of rGO is flat, entangled and almost transparent morphology. This morphology is due to the ultrathin character of the rGO nanosheets. Fig. 3c shows the morphology of carbon nanotubes. This CNT consists of multiwalled nanotubes with hallow internal channel at the tip. In Fig. 3d, rGO-CNT presents a few-layered graphene sheet, coupled with a carbon nanotube. The average diameter of carbon nanotube was 14 nm. The mixture of rGO and CNT morphology confirmed the hybridization of the nanocomposite.

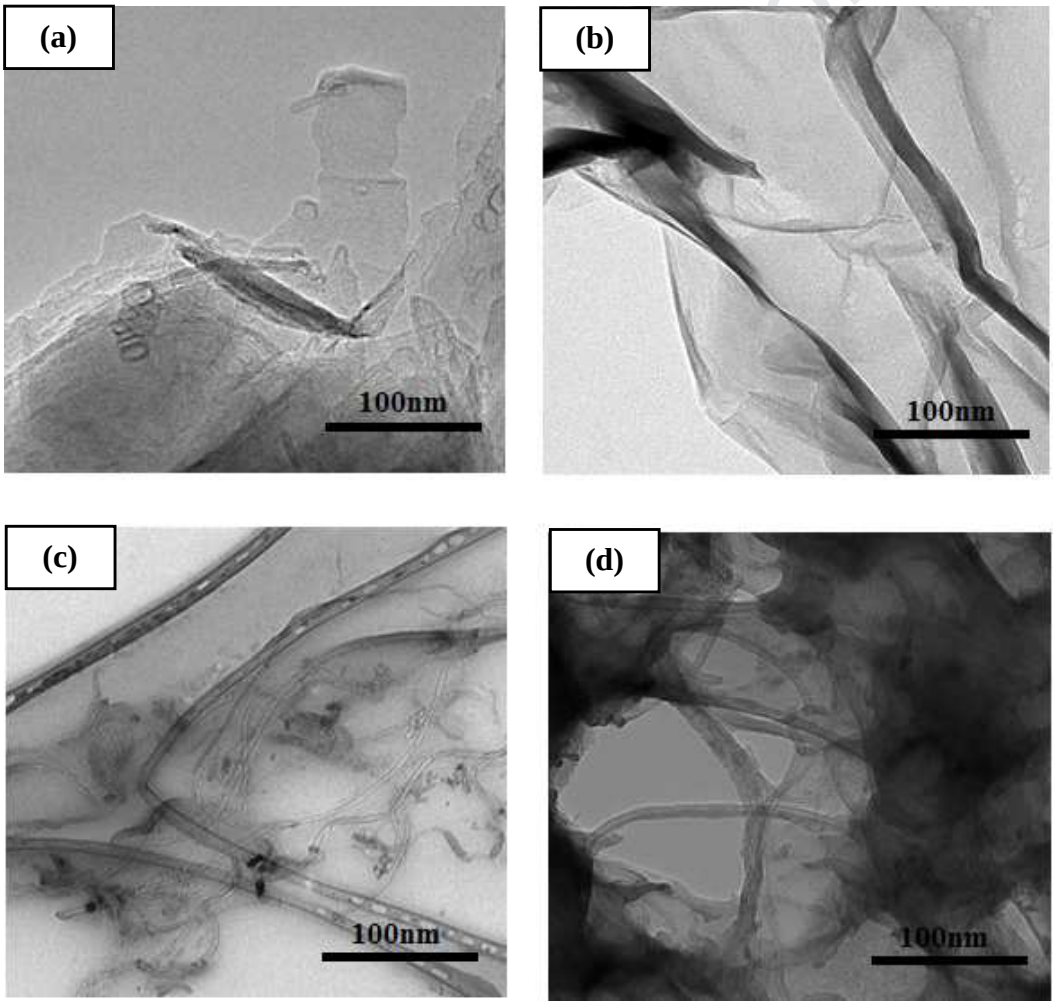

Fig. 3. The TEM images of the synthesized (a) GO, (b) rGO, (c) CNT and (d) rGO-CNT.

3.2 Electrochemical characterization of ssDNA/rGO-CNT/GCE bioelectrode

3.2.1 Optimization of working electrodes

Two main parameters have been optimized in this study to achieve the best sensing performance of our developed electrode. Firstly, the concentration effect of rGO-CNT on the electrodes was investigated as shown in Figure 4(a). The current density increased with the increasing concentration from 1 to 11 mg mL^{-1} and reached the maximum current density at 5 mg mL^{-1} of rGO-CNT. The current density decreased drastically when the loading amount exceeded 5 mg mL^{-1}. This phenomenon was due to the development of thick layers on the surface of electrodes which block the electron from reaching the electrode and thus lowering its sensitivity. Lastly, the concentration of rGO-CNT was optimized to 5 mg mL^{-1}.

The effect of aptamer concentration loaded on the rGO-CNT electrode was also optimized as shown in Figure 4(b). As the aptamer concentration increased from 1 to 20 µmol L^{-1}, the current density also increased. However, with further increase in aptamer concentration, the increase in current density was almost constant because the aptamer fixed on the electrode has reached a saturation point. Therefore, 5 µmol L^{-1} of aptamer concentration was selected for subsequent experiments.

The electrochemical characterization of the developed electrode using Cyclic voltammetry in Zobell's solution at 100 mVs^{-1} scan rate is shown in Figure 4(c). A pair of redox peaks was detected for bare GCE electrode. A slight increase in redox peak current, upon the coating of rGO on the electrode's surface was observed. Subsequently, the redox peak current for rGO-CNT/GCE is higher than rGO/GCE and bare GCE. This can be attributed to the uniform attachment of CNT on rGO surface which provides a high surface area and excellent electron transfer which enhances the overall conductivity [33].

After immobilization of aptamer, the peak current increased significantly due to the interactions of negatively charged DNA on the electrode surface contributes to ionic conductance and increases the overall charge transfer [34].

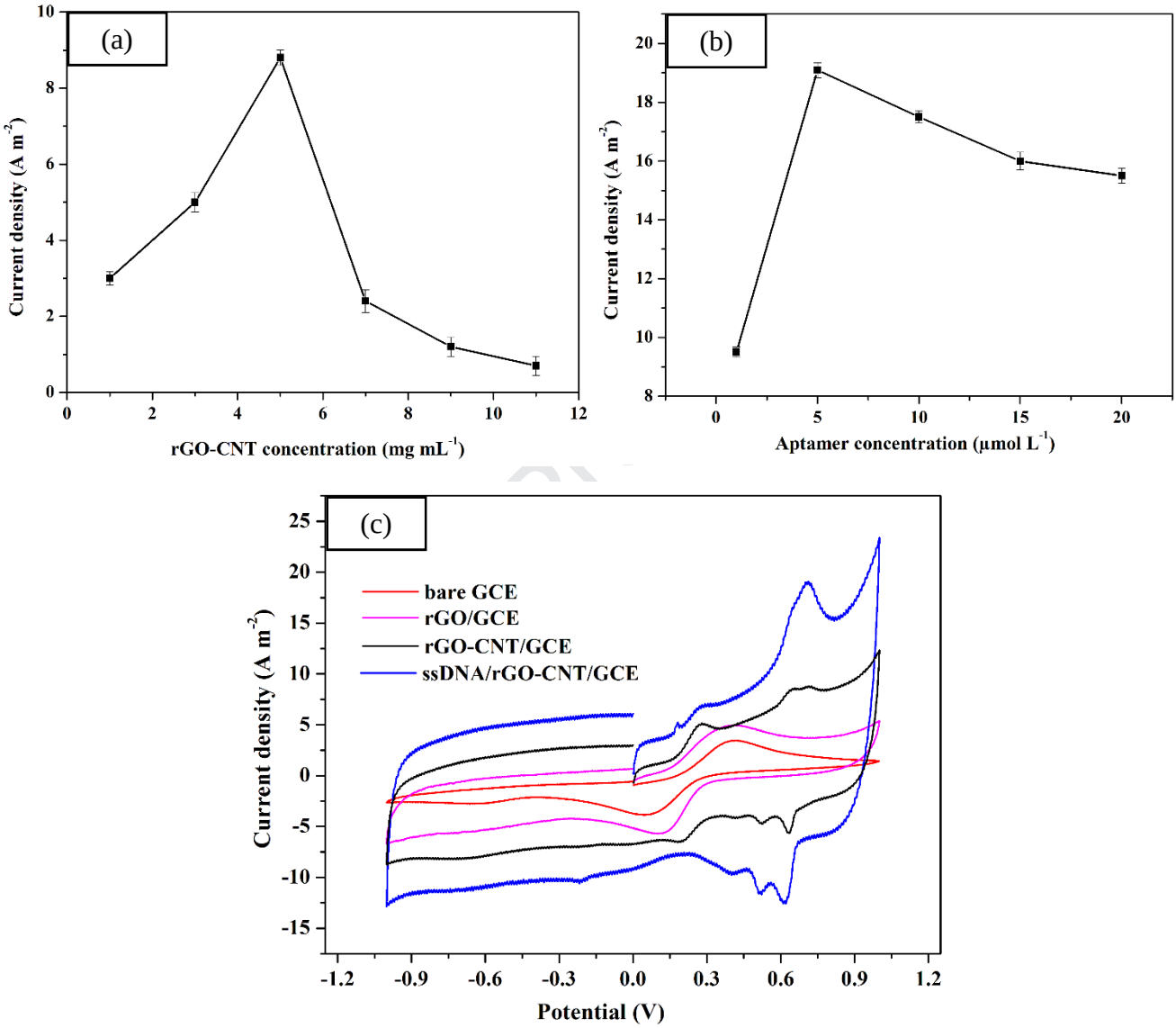

Fig.4. The effects of (a) rGO-CNT concentrations (mg mL^{-1}), (b) aptamer concentrations (µmol L^{-1}) and (c) electrochemical properties of the fabricated electrodes. The CV of bare GCE, rGO/GCE, rGO-CNT/GCE, and ssDNA/rGO-CNT/GCE, in Zobell solution (pH 7.0) at 100 mVs^{-1} scan rate.

3.3 Sensitivity test

The electrochemical detection ability of the rGO-CNT nanocomposite was studied by exposing the aptamer-modified ssDNA/rGO-CNT/GCE electrode (aptasensor) to the bacterial concentration (10^1 to 10^8 cfu mL^{-1}). Fig. 5(A) shows that the current density increases with increasing concentrations of *Salmonella* cells. There is a notable change in the electrochemical behaviour of each assembly step in the aptasensor preparation that could be observed from the DPV response at 100 mVs^{-1} scan rate. A prominent oxidation peak for the rGO-CNT/GCE can be observed at the potential of 0.23 V indicating excellent electron transferability and good electrical conductivity of rGO-CNT nanocomposite. After immobilization of aptamer, a large increase in oxidation current density of ssDNA/rGO-CNT/GCE is visible in the voltammogram. This is due to the increase in charge transfer as a result of the ionic conductance and π-π DNA interaction which proves the binding of aptamer on the rGO-CNT surface with high affinity [35]. In the presence of bacteria, the oxidation peak current increased proportionally to the concentration of bacteria cells. Nevertheless, the current decreased prominently as compared to ssDNA/rGO-CNT/GCE after binding of bacterial onto the electrode's surface. This is ascribed to the negatively charged cell membrane that creates hindrances and blocks the electron transfer to the electrode surface [36]. When the bacterial concentration increased, the current density also increased due to the kinetics of interfacial electron-transfer and increase in the electron-transfer resistance from the medium to the electrode's surface. This causes an electro-permeation of conductive ions from inside the bacterial cells into the electrolyte [37]. More bacteria cells cause leakage of more conductive ions which increases the current density.

The plot of current density vs. the logarithm of the concentration of bacteria (Fig. 5B) showed a linear relationship with a correlation coefficient of 0.9855. The limit of detection of this sensor was 10^1 cfu mL^{-1}.

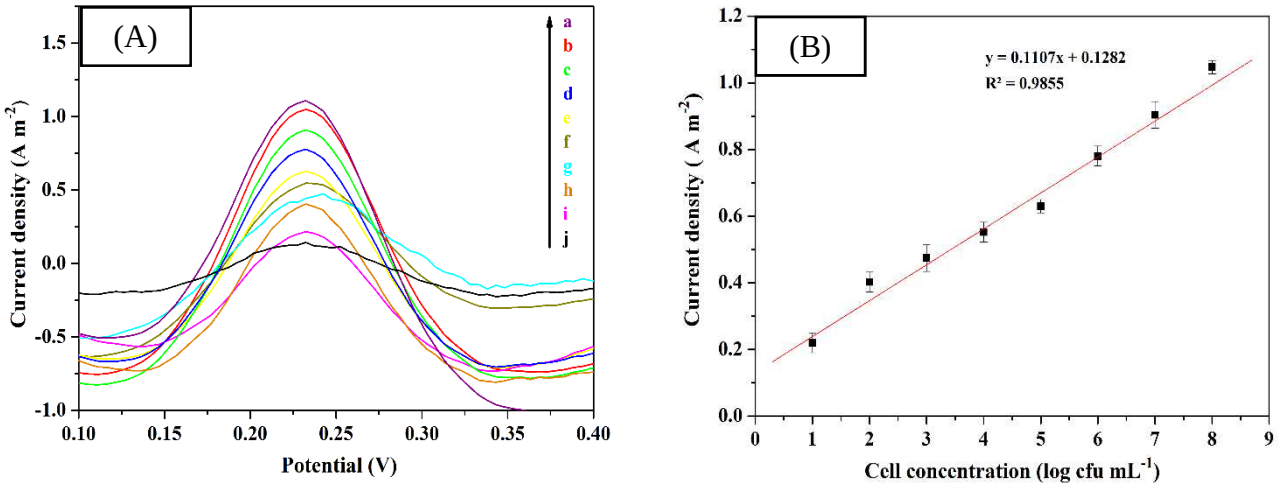

Fig.5. Evaluation of sensitivity of aptasensor on a different *S.* Typhimurium concentration. (A) DPV of (a) ssDNA/rGO-CNT/GCE, (b) 10^8 cfu mL^{-1}, (c) 10^7 cfu mL^{-1} (d) 10^6 cfu mL^{-1}, (e) 10^5 cfu mL^{-1}, (f) 10^4 cfu mL^{-1}, (g) 10^3 cfu mL^{-1}, (h) 10^2 cfu mL^{-1}, (i) 10^1 cfu mL^{-1} and (j) rGO-CNT/GCE in 0.1 mol L^{-1} of KCl solution containing 3 mmol L^{-1} $K_3[Fe(CN)_6]$ at pulse height 50 mV, pulse width 70 ms.(B) The graph depicts linear relationship between current density and cell concentration (logarithm).

3.4 Selectivity and specificity tests

The selectivity and specificity tests were studied using bacteria concentrations of 10^2 cfu mL^{-1}. Fig. 6(a) shows the selectivity test of the aptamer against other serovars of *Salmonella enterica* such as *S.* Albany, *S.* Enteritidis, *S.* Weltevreden, *S.* Typhi, and *S.* Derby. All the bacteria exhibited peak currents like *S.* Typhimurium which indicated the aptamer was specific for all tested *Salmonella* serovars. Nevertheless, when the aptasensor was tested against non-*Salmonella* bacteria (*E. coli*, *K. pneumoniae*, *P. aeruginosa*, *S. aureus* and *Enterococcus faecalis*), the current density was lower than that of the limit of detection (LOD) of the electrode (Fig. 6(b)). This indicates non-specificity of the aptamer to non-

Salmonella bacterial cells. The intermolecular folding of aptamers enables them to identify and bind to their targets with good affinity and specificity discriminating the binding with non-*Salmonella* bacteria.

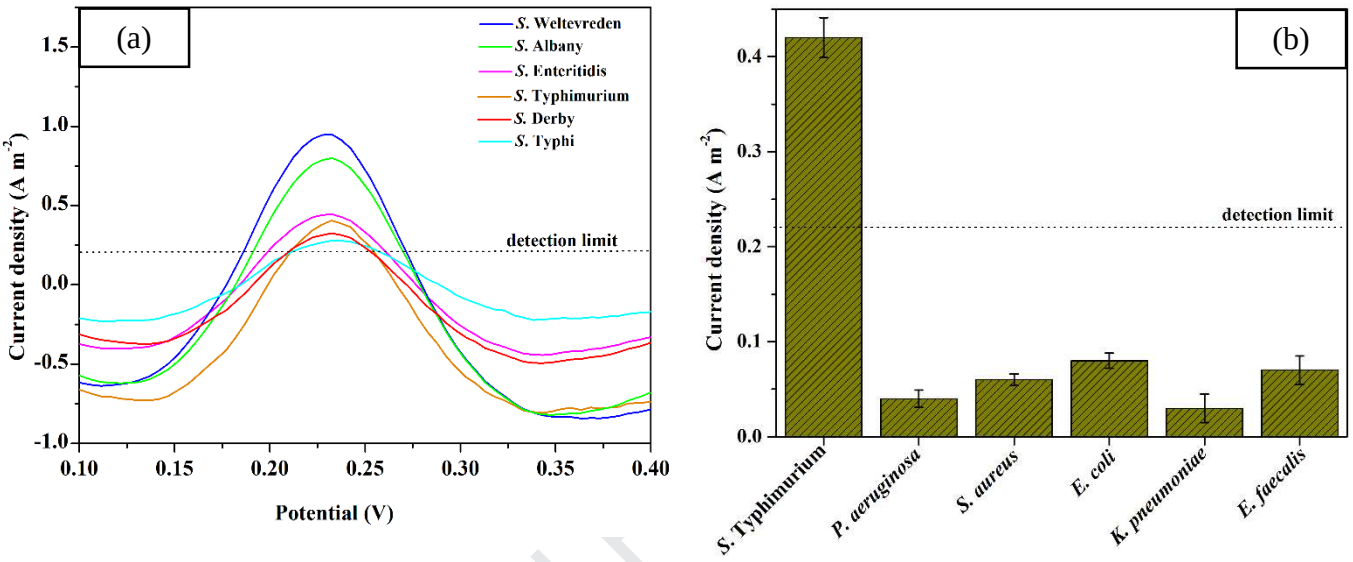

Fig.6. Selectivity and specificity evaluation of the aptasensor in detecting different bacterial strains. (a) DPV of *S.* Weltevreden, *S.* Albany, *S.* Enteritidis, *S.* Typhimurium, *S.* Derby and *S.* Typhi in 0.1 mol L^{-1} KCl solution with 3 mmol L^{-1} of $K_3[Fe(CN)_6]$] at pulse height of 50 mV, pulse width of 70 ms. (b) Specificity of aptasensor in various samples. Data are expressed as the mean ± standard deviation (n = 3).

The performance of the developed rGO-CNT aptasensor for bacteria detection was compared to previous studies and the important characters are summarized in Table 1. The obtained LOD was much lower using the prepared biosensor in this study compared to those published data. The comparison table shows that the developed rGO-CNT aptasensor exhibited high sensitivity with improved detection limit. Hence this provides an alternative approach for rapid detection of *S.* Typhimurium.

Table 1. A comparison of different methods of bacterial detection with the current study.

Materials	Targeted bacteria	Detection methods	LOD (cfu mL^{-1})	Time	Ref
rGO-MWCNT	*Salmonella*	EIS	25	1 h	[38]
CNT	*S. aureus*	Potentiometry	8×10^2	Not stated	[39]
rGO-Au	*S. aureus*	EIS	10	Not stated	[40]
-	*Salmonella* spp.	Multiplex-PCR	10^3	3 h	[41]
Gold Nanoparticle-Based Enzyme-Linked Antibody	*S.* Typhimurium	Immunological assay	10^3	2 h	[42]
Three-Dimensional Interdigitated Electrode Array (3D-IDEA)	*E. coli* O157:H7	EIS	2.9×10^2	30 min	[43]
rGO-CNT	*S.* Typhimurium	DPV	10^1	10 min	This work

3.5 Reproducibility and stability properties of the aptasensor

Under the optimal conditions, the electrochemical reproducibility and stability of rGO-CNT nanocomposite (data not shown) were investigated by repetitive cycling procedure (21 cycles), which was observed to produce changes that were insignificant for the peak current density. Also, ssDNA/rGO-CNT/GCE was stored for 20 days in ultrapure water at 4 °C and it showed good to excellent stability as an aptasensor. The slight decrease in signal was noted at day 20 and therefore the aptasensor has good storage stability.

3.6 Food samples evaluation

Fig. 7 shows the response of the aptasensor with five chicken meat samples. Out of 5 chicken meat samples, 3 chicken samples (CS1, CS2, CS3) exhibited a positive response to the presence of different concentration of *Salmonella* ranging from 10^1 to 10^3 cfu mL^{-1} while another two samples (CS 4 and CS5) gave a response below the detection limit. When the same food samples were tested using the conventional culture method, presumptive *Salmonella* isolates were detected on Brilliance™ Salmonella agar (Oxoid) for samples CS1, CS2 and CS3 only (Data not shown). Hence the data obtained by the aptasensor was validated by the culture method. The results obtained in this food sample analysis were comparable to the standard graph obtained in Fig. 5(B). This aptasensor showed good recovery illustrating its applicability for food sample analysis.

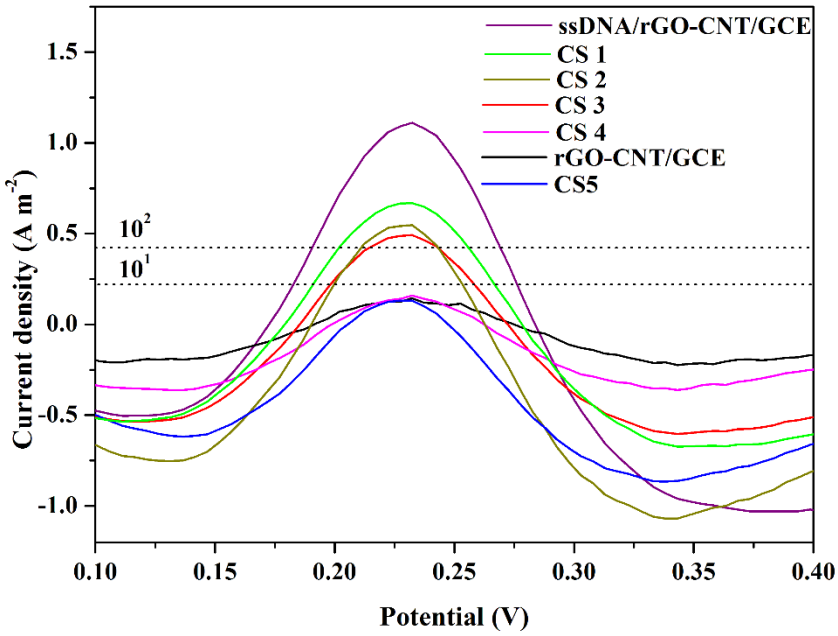

Fig.7. DPV comparison between bacterial detection in five different chicken samples with rGO-CNT/GCE and ssDNA/rGO-CNT/GCE. Food samples: CS1 – CS5

4 Conclusion

In summary, an electrochemical aptasensor rGO-CNT nanocomposite for the detection of *Salmonella* was successfully developed. The nanocomposite has been characterized by physicochemical methods to show the hybridization of rGO and CNT. The incorporated amino-modified DNA aptamer to the rGO-CNT successfully detected whole *Salmonella* bacterial cells without any pre-treatment or DNA extraction steps. The complete working electrode ssDNA/rGO-CNT/GCE demonstrated significant current peaks for various concentrations of *S.* Typhimurium ranging from 10^1 until 10^8 cfu mL^{-1} with a LOD value of 10^1 cfu mL^{-1}. More remarkably, the detection of *Salmonella* was able to be completed in 10 min. Furthermore, the prepared aptasensor successfully distinguished *Salmonella* from non-*Salmonella* cells. The overall results indicated that the rGO-CNT nanocomposite exhibited good electrochemical activity attributed to the presence of reduced graphene oxide which synergistically improves electron transfer. Moreover, the carbon nanotube has acted as the spacer and provided a large specific surface area for aptamer immobilization. Thus, the designed ssDNA/rGO-CNT/GCE showed high selectivity, sensitivity and specificity, cost-effective approach for foodborne pathogen analysis. Nevertheless, there are some limitation which must be considered for the development of the aptasensor such as pH, ionic strength, viscosity and temperature. Thus, in future study, more focus will be given on the design of aptasensors against unexplored target analyte with different types of aptamer.

Acknowledgement

This study was supported by Trans-Disciplinary Research Grant Scheme (TRGS) through Grant No. TR002C-2014B, TR002A-2014B and TR002B-2014B from Ministry of Higher

Education, Malaysia. We thank Lim Teck Wei for assistance in the food microbiology analysis.

Compliance with Ethical Standards:

Funding: This work was funded by the Ministry of Higher Education (MOHE), Malaysia and University of Malaya through Trans-disciplinary Research Grant Scheme (TRGS) under Grant number TR002C-2014B, TR002A-2014B and TR002B-2014B.

Conflict of Interest: Jimmy Nelson Appaturi, Kwai Lin Thong, Thiruchelvi Pulingam, Shalini Muniandy, Noraini Binti Ahmad and Bey Fen Leo declare that there are no conflict of interest.

Ethical approval: This article does not contain information from any studies that were carried out with human or animals.

Informed consent: No informed consent was obtained as human participants were not involved in this work.

References

1. Muniandy S, Dinshaw IJ, Teh SJ, Lai CW, Ibrahim F, Thong KL, Leo BF (2017) Graphene-based label-free electrochemical aptasensor for rapid and sensitive detection of foodborne pathogen. Anal Bioanal Chem 409 (29):6893-6905. doi:10.1007/s00216-017-0654-6

2. Ngoi ST, Teh CSJ, Chai LC, Thong KL (2015) Overview of molecular typing tools for the characterization of Salmonella enterica in Malaysia. Biomedical and Environmental Sciences 28 (10):751-764

3. Ma X, Xu X, Xia Y, Wang Z (2018) SERS aptasensor for Salmonella typhimurium detection based on spiny gold nanoparticles. Food Control 84:232-237. doi:https://doi.org/10.1016/j.foodcont.2017.07.016

4. Ranjbar S, Shahrokhian S, Nurmohammadi F (2018) Nanoporous gold as a suitable substrate for preparation of a new sensitive electrochemical aptasensor for detection of Salmonella typhimurium. Sensors and Actuators B: Chemical 255:1536-1544. doi:https://doi.org/10.1016/j.snb.2017.08.160

5. Srisa-Art M, Boehle KE, Geiss BJ, Henry CS (2017) Highly Sensitive Detection of Salmonella typhimurium Using a Colorimetric Paper-Based Analytical Device Coupled with Immunomagnetic Separation. Analytical chemistry 90 (1):1035-1043

6. Lee K-M, Runyon M, Herrman TJ, Phillips R, Hsieh J (2015) Review of Salmonella detection and identification methods: aspects of rapid emergency response and food safety. Food Control 47:264-276

7. Silva NFD, Magalhães JMCS, Freire C, Delerue-Matos C (2018) Electrochemical biosensors for Salmonella: State of the art and challenges in food safety assessment. Biosensors and Bioelectronics 99:667-682. doi:https://doi.org/10.1016/j.bios.2017.08.019
8. Schoukroun-Barnes LR, Macazo FC, Gutierrez B, Lottermoser J, Liu J, White RJ (2016) Reagentless, structure-switching, electrochemical aptamer-based sensors. Annual Review of Analytical Chemistry 9:163-181
9. Meng H-M, Liu H, Kuai H, Peng R, Mo L, Zhang X-B (2016) Aptamer-integrated DNA nanostructures for biosensing, bioimaging and cancer therapy. Chemical Society Reviews 45 (9):2583-2602
10. Sefah K, Shangguan D, Xiong X, O'donoghue MB, Tan W (2010) Development of DNA aptamers using Cell-SELEX. Nature protocols 5 (6):1169
11. Dinshaw IJ, Muniandy S, Teh SJ, Ibrahim F, Leo BF, Thong KL (2017) Development of an aptasensor using reduced graphene oxide chitosan complex to detect Salmonella. Journal of Electroanalytical Chemistry 806:88-96. doi:https://doi.org/10.1016/j.jelechem.2017.10.054
12. Palchetti I, Mascini M (2015) Electrochemical Nucleic Acid Aptamer–Based Biosensors. Electrochemical Biosensors:75
13. Ansari N, Yazdian-Robati R, Shahdordizadeh M, Wang Z, Ghazvini K (2017) Aptasensors for quantitative detection of Salmonella Typhimurium. Analytical Biochemistry 533:18-25. doi:https://doi.org/10.1016/j.ab.2017.06.008
14. Joshi R, Janagama H, Dwivedi HP, Kumar TS, Jaykus L-A, Schefers J, Sreevatsan S (2009) Selection, characterization, and application of DNA aptamers for the capture and detection of Salmonella enterica serovars. Molecular and cellular probes 23 (1):20-28
15. Chen A, Chatterjee S (2013) Nanomaterials based electrochemical sensors for biomedical applications. Chemical Society Reviews 42 (12):5425-5438
16. Wang Z, Yu J, Gui R, Jin H, Xia Y (2016) Carbon nanomaterials-based electrochemical aptasensors. Biosensors and Bioelectronics 79:136-149
17. Pumera M (2010) Graphene-based nanomaterials and their electrochemistry. Chemical Society Reviews 39 (11):4146-4157
18. Liu W-W, Chai S-P, Mohamed AR, Hashim U (2014) Synthesis and characterization of graphene and carbon nanotubes: a review on the past and recent developments. Journal of Industrial and Engineering Chemistry 20 (4):1171-1185
19. Toda K, Furue R, Hayami S (2015) Recent progress in applications of graphene oxide for gas sensing: a review. Analytica chimica acta 878:43-53
20. Goenka S, Sant V, Sant S (2014) Graphene-based nanomaterials for drug delivery and tissue engineering. Journal of Controlled Release 173:75-88
21. Liu Y, Dong X, Chen P (2012) Biological and chemical sensors based on graphene materials. Chemical Society Reviews 41 (6):2283-2307
22. Raccichini R, Varzi A, Passerini S, Scrosati B (2015) The role of graphene for electrochemical energy storage. Nature materials 14 (3):271
23. Badhulika S, Terse-Thakoor T, Chaves Villarreal CM, Mulchandani A (2015) Graphene hybrids: synthesis strategies and applications in sensors and sensitized solar cells. Frontiers in chemistry 3:38
24. Mani V, Chen S-M, Lou B-S (2013) Three dimensional graphene oxide-carbon nanotubes and graphene-carbon nanotubes hybrids. Int J Electrochem Sci 8 (11641):e60
25. Heydari-Bafrooei E, Shamszadeh NS (2017) Electrochemical bioassay development for ultrasensitive aptasensing of prostate specific antigen. Biosens Bioelectron 91:284-292
26. Rostamabadi PF, Heydari-Bafrooei E (2019) Impedimetric aptasensing of the breast cancer biomarker HER2 using a glassy carbon electrode modified with gold nanoparticles in a composite consisting of electrochemically reduced graphene oxide and single-walled carbon nanotubes. Microchimica Acta 186 (8):495

27. Heydari-Bafrooei E, Askari S (2017) Ultrasensitive aptasensing of lysozyme by exploiting the synergistic effect of gold nanoparticle-modified reduced graphene oxide and MWCNTs in a chitosan matrix. Microchimica Acta 184 (9):3405-3413
28. Joshi R, Janagama H, Dwivedi HP, Senthil Kumar TMA, Jaykus L-A, Schefers J, Sreevatsan S (2009) Selection, characterization, and application of DNA aptamers for the capture and detection of Salmonella enterica serovars. Mol Cell Probes 23 (1):20-28. doi:https://doi.org/10.1016/j.mcp.2008.10.006
29. Singh A, Sinsinbar G, Choudhary M, Kumar V, Pasricha R, Verma HN, Singh SP, Arora K (2013) Graphene oxide-chitosan nanocomposite based electrochemical DNA biosensor for detection of typhoid. Sensors and Actuators B: Chemical 185:675-684. doi:https://doi.org/10.1016/j.snb.2013.05.014
30. Hasan MR, Pulingam T, Appaturi JN, Zifruddin AN, Teh SJ, Lim TW, Ibrahim F, Leo BF, Thong KL (2018) Carbon nanotube-based aptasensor for sensitive electrochemical detection of whole-cell Salmonella. Anal Biochem 554:34-43. doi:https://doi.org/10.1016/j.ab.2018.06.001
31. Tan L-L, Ong W-J, Chai S-P, Mohamed AR (2013) Reduced graphene oxide-TiO(2) nanocomposite as a promising visible-light-active photocatalyst for the conversion of carbon dioxide. Nanoscale Research Letters 8 (1):465-465. doi:10.1186/1556-276X-8-465
32. Mishra SK, Tripathi SN, Choudhary V, Gupta BD (2014) SPR based fibre optic ammonia gas sensor utilizing nanocomposite film of PMMA/reduced graphene oxide prepared by in situ polymerization. Sensors and Actuators B: Chemical 199:190-200. doi:https://doi.org/10.1016/j.snb.2014.03.109
33. Zhu Z (2017) An Overview of Carbon Nanotubes and Graphene for Biosensing Applications. Nano-Micro Letters 9 (3):25. doi:10.1007/s40820-017-0128-6
34. R Johnson R, Johnson atc, L Klein M (2008) Probing the Structure of DNA−Carbon Nanotube Hybrids with Molecular Dynamics, vol 8. doi:10.1021/nl071909j
35. Johnson RR, Johnson ATC, Klein ML (2008) Probing the Structure of DNA−Carbon Nanotube Hybrids with Molecular Dynamics. Nano Letters 8 (1):69-75. doi:10.1021/nl071909j
36. Labib M, Zamay AS, Kolovskaya OS, Reshetneva IT, Zamay GS, Kibbee RJ, Sattar SA, Zamay TN, Berezovski MV (2012) Aptamer-Based Viability Impedimetric Sensor for Bacteria. Anal Chem 84 (21):8966-8969. doi:10.1021/ac302902s
37. Varshney M, Li Y (2007) Interdigitated array microelectrode based impedance biosensor coupled with magnetic nanoparticle–antibody conjugates for detection of Escherichia coli O157:H7 in food samples. Biosens Bioelectron 22 (11):2408-2414. doi:https://doi.org/10.1016/j.bios.2006.08.030
38. Jia F, Duan N, Wu S, Dai R, Wang Z, Li X (2016) Impedimetric salmonella aptasensor using a glassy carbon electrode modified with an electrodeposited composite consisting of reduced graphene oxide and carbon nanotubes. Microchimica Acta 183 (1):337-344
39. Zelada-Guillén GA, Sebastián-Avila JL, Blondeau P, Riu J, Rius FX (2012) Label-free detection of Staphylococcus aureus in skin using real-time potentiometric biosensors based on carbon nanotubes and aptamers. Biosens Bioelectron 31 (1):226-232. doi:https://doi.org/10.1016/j.bios.2011.10.021
40. Jia F, Duan N, Wu S, Ma X, Xia Y, Wang Z, Wei X (2014) Impedimetric aptasensor for Staphylococcus aureus based on nanocomposite prepared from reduced graphene oxide and gold nanoparticles. Microchimica Acta 181 (9):967-974. doi:10.1007/s00604-014-1195-8
41. Wang L, Li Y, Mustapha A (2007) Rapid and simultaneous quantitation of Escherichia coli O157: H7, Salmonella, and Shigella in ground beef by multiplex real-time PCR and immunomagnetic separation. J Food Prot 70 (6):1366-1372

42. Wu W, Li J, Pan D, Li J, Song S, Rong M, Li Z, Gao J, Lu J (2014) Gold nanoparticle-based enzyme-linked antibody-aptamer sandwich assay for detection of Salmonella Typhimurium. ACS applied materials & interfaces 6 (19):16974-16981
43. Brosel-Oliu S, Ferreira R, Uria N, Abramova N, Gargallo R, Muñoz-Pascual F-X, Bratov A (2018) Novel impedimetric aptasensor for label-free detection of Escherichia coli O157:H7. Sensors and Actuators B: Chemical 255:2988-2995. doi:https://doi.org/10.1016/j.snb.2017.09.121

Research Highlights

- rGO-CNT nanocomposite was developed for detection of *Salmonella.*
- rGO-CNT nanocomposite demonstrating the synergistic effect.
- Detection limit of 10^1 cfu mL^{-1} for *S.* Typhimurium.
- A sensitive, selective and specific aptasensor with a wide detection range was produced.
- The ssDNA/rGO-CNT/GCE was successfully applied to real food samples.